

Explanatory Notes: Source Parameter Determination:

The calculations of magnitudes over a grid of trial source locations (Bakun and Wentworth, 1997) are based on an empirical intensity attenuation relation (Fäh et al., 2003). The calibration relations are:

For shallow earthquake sources (~ 10 km depth):

$$\begin{aligned} M_i &= [I_i - 0.096 + 0.043d_i] / 1.27 && \text{(for } d_i < 70\text{km)} \\ M_i &= [I_i + 1.93 + 0.0064d_i] / 1.27 && \text{(for } d_i > 70\text{km)} \end{aligned}$$

For deep earthquake sources (~ 10 km depth):

$$\begin{aligned} M_i &= [I_i + 1.73 + 0.030d_i] / 1.44 && \text{(for } d_i < 70\text{km)} \\ M_i &= [I_i + 3.04 + 0.0064d_i] / 1.44 && \text{(for } d_i > 70\text{km)} \end{aligned}$$

M_i is the moment magnitude estimates, I_i the EMS98 Intensity value at site i , and d_i the distance (km) from the source location to site i . I_i was set to 7 for all sites of lacustrine landslides in Lakes Zurich and Lucerne, as this is the accepted threshold intensity for basinwide landsliding calibrated with historic earthquakes in Central Switzerland (Monecke et al., 2004). To account for uncertainties of the threshold values of macroseismic intensity for basin wide landsliding and to estimate a lower bound for the calculated magnitude in our study we also applied a more conservative threshold values of 6.5 in the grid search calculations which reduces the resulting magnitude estimates by about 0.3 magnitude units. For high magnitudes ($M > 6$) the empirical intensity attenuation relation for shallow earthquake sources is not well established because calibration events with $M > 5.5$ are rare. However, sensitivity analyses of uncertainties related to the hypocenter depth location are relatively small (e.g. applying the attenuation relationship for a deep source south of the NAF rather than a shallow source would only increase magnitude estimates in the near epicentral distance (< 20 km) by ~ 0.2 magnitude units).

2006221

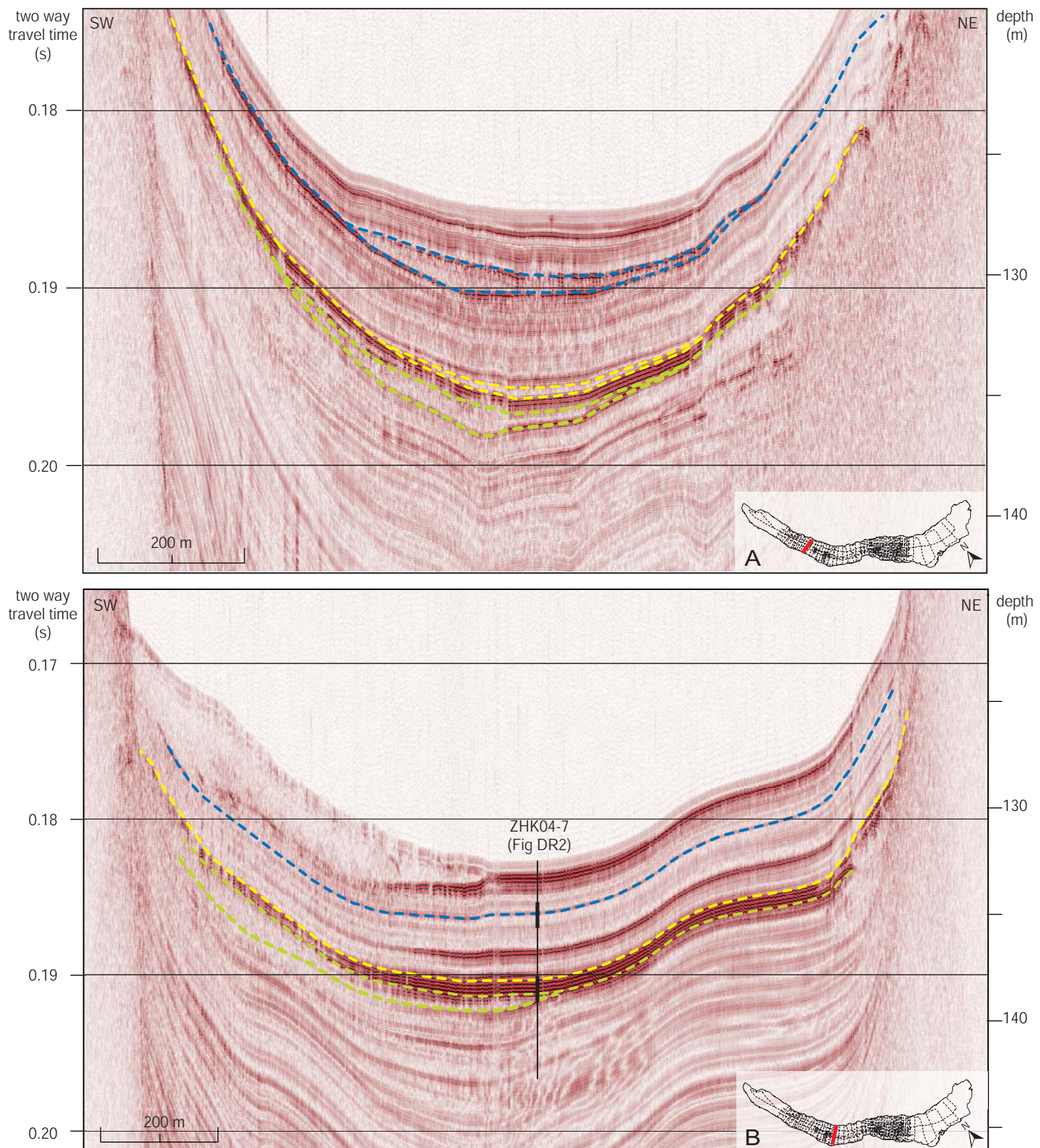


Figure DR1: Two of the total 127 (see insets in the lower right corner) 3.5 kHz seismic profiles showing the subsurface of Lake Zurich where we identify the mass movement deposits due to their chaotic-to-transparent seismic facies and their characteristic onlap geometries. Dashed lines show the three seismostratigraphic horizons and their corresponding landslide deposits. Blue, yellow and green correspond to the 2200 ± 55 , $11,530 \pm 185$ and $13,840 \pm 145$ cal yr B.P. event, respectively, where multiple simultaneous slope failures occurred throughout the lake basin. b) Seismic profile with location of core ZHK04-7. Intervals marked with bold lines are shown as photographs in Figure DR2. Note prominent mass-movement deposit in the uppermost part on the left side. It corresponds to the 1875 A.D. landslide triggered by human construction along the shore (Kelts, 1980).

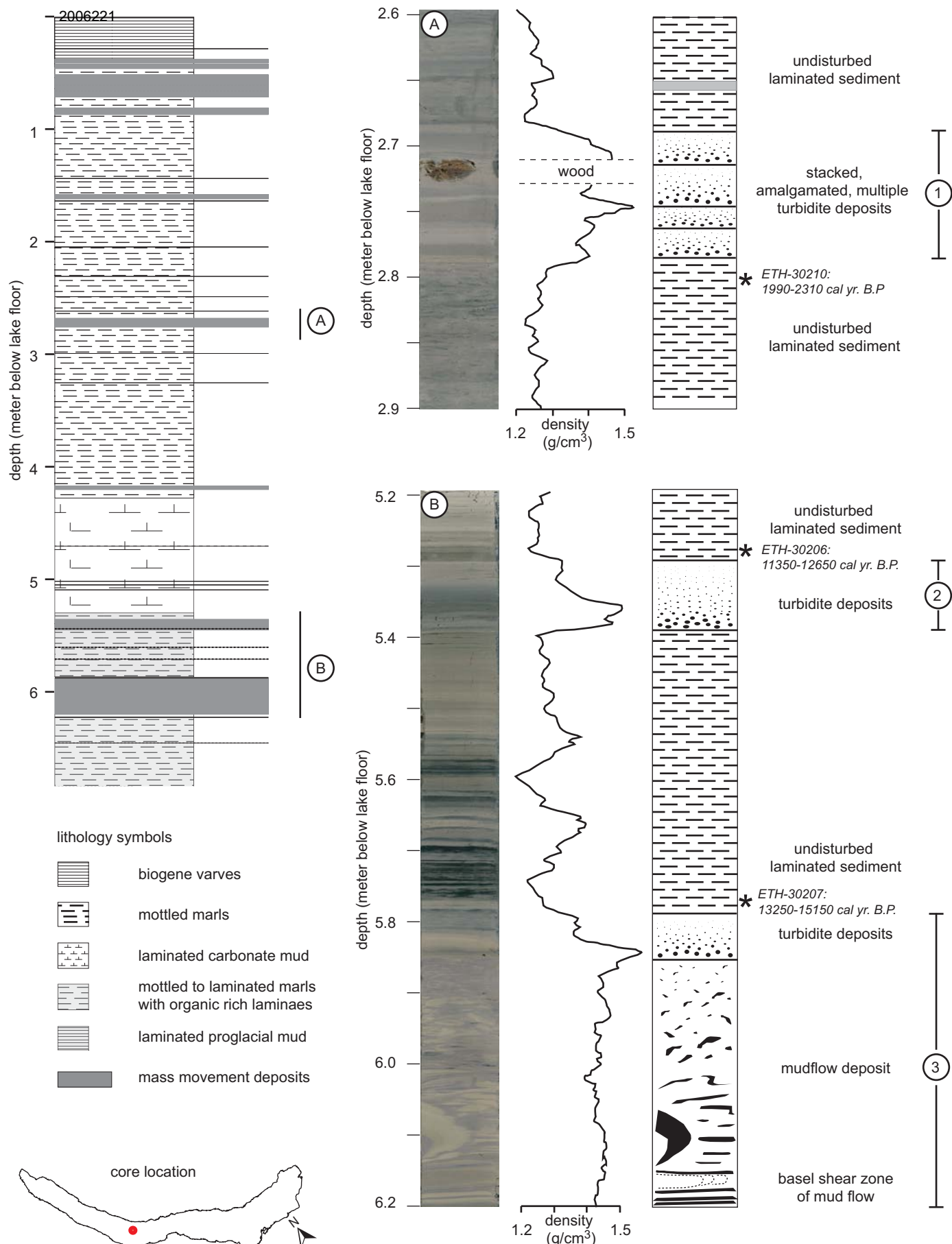


Figure DR2: Lithologic profile, bulk density log and core photos (by Urs Gerber) at two specific sections (A and B) from gravity piston core ZHK04-7 retrieved from the deepest central part of Lake Zurich. It shows the distinct sedimentologic "fingerprint" (i.e. mass flow deposits and turbidite deposits) of sublacustrine slope failures triggered by the three major paleo-earthquakes (numbered from 1 to 3). * indicate position of AMS ^{14}C sample (see table DR1).

Table DR1. ^{14}C ages and calibration of samples used to date the prehistoric event horizons (Table S2)

Core Nr.	Location ⁽¹⁾	Depth in core (m)	Sample Nr.	Sample age ⁽²⁾ (^{14}C yr B.P.)	Sample age ⁽³⁾ (cal. yr B.P.)	$\delta^{13}\text{C}$ (‰)	material
ZHK04-7	688526 / 236159	5.32	ETH-30206	10230 ± 85	11350 - 12650	-27.7 ± 1.2	leaf remains
ZHK04-7	688526 / 236159	5.76	ETH-30207	11710 ± 100	13250 - 15150	-26.7 ± 1.2	wood
ZHK04-7	688526 / 236159	2.81	ETH-30210	2135 ± 55	1990 - 2310	-32.2 ± 1.2	leaf remains
ZHK04-5	699687 / 230486	3.78	ETH-30215	8995 ± 80	9750 - 10400	-27.4 ± 1.2	leaf remains
ZHK04-1	685585 / 240583	1.195	ETH-30711	1585 ± 50	1340 - 1570	-26.5 ± 1.2	leaf remains
ZHK04-1	685585 / 240583	2.395	ETH-30712	3230 ± 50	3350 - 3580	-29.2 ± 1.2	leaf remains
ZHK04-5	699687 / 230486	4.12	ETH-30715	11560 ± 90	13150 - 13950	-25.3 ± 1.2	wood
Zübo 1980 ⁽⁴⁾	687615 / 237266	5.75	GL8 ⁽⁸⁾	9990 ± 150	11058 - 11975	-	wood
Zübo 1980 ⁽⁴⁾	687615 / 237266	7.5	GL11 ⁽⁸⁾	12800 ± 250	14000 - 15595	-	wood
LST ⁽⁵⁾	-	-	Tephra	11,230 ± 40	13003 - 13755	-	

⁽¹⁾ Location is given in Swiss Grid (CH1903) Coordinates.⁽²⁾Dating by AMS (accelerator mass spectrometry) with the tandem accelerator at the Institute of Particle Physics at the Swiss Federal Institute of Technology Zurich (ETH).⁽³⁾Calibration (2σ range) was carried out applying the Intercal98-calibration curve (Stuiver and Reimer, 1993).⁽⁴⁾ Dates by Lister (1988).⁽⁵⁾ Laacher See Tephra (LST), radiocarbon dated by Hajdas et al. (1995).

Table DR2. Dating of prehistoric event

Sample Nr.	Sample age ⁽¹⁾ (¹⁴ C yr B.P.)	Sample age ⁽²⁾ (cal. yr B.P.)	Offset ⁽³⁾ (cm)	Sed.rate ⁽⁴⁾ (cm/yr)	Horizon age (cal. yr B.P.)	Horizon age (overlap range) (cal. yr B.P.)	Center of overlap ⁽⁵⁾ (cal. yr B.P.)
<u>Event horizon 1</u>							
ETH-30711	1585 ± 50	1340 - 1570	-37	0.05	2082 - 2312		
ETH-30712	3230 ± 50	3350 - 3580	60	0.05	2147 - 2377		
ETH-30210	2135 ± 55	1990 - 2310	3	0.06	1937 - 2257	2147 - 2257	2200
<u>Event horizon 2</u>							
ETH-30206	10230 ± 85	11350 - 12650	-	0.02	11350 - 12650		
ETH-30215	8995 ± 80	9750 - 10400	-14	0.01	11109 - 11759		
LST ⁽⁶⁾	11230 ± 40	13003 - 13755	21	0.01	10964 - 11716		
GL8 ⁽⁷⁾	9990 ± 150	11058 - 11975	-	-	11058 - 11975	11350 - 11716	11530
<u>Event horizon 3</u>							
LST ⁽⁶⁾	11230 ± 40	13003 - 13755	-12	0.04	13304 - 14056		
ETH-30207	11710 ± 100	13250 - 15150	-3	0.04	13325 - 15225		
ETH-30715	11560 ± 90	13150 - 13950	-5	0.03	13317 - 14117		
LST ⁽⁶⁾	11230 ± 40	13003 - 13755	-7	0.03	13236 - 13988		
GL11 ⁽⁷⁾	12800 ± 250	14000 - 15595	15	0.05	13700 - 15295	13700 - 13988	13840

⁽¹⁾Dating by AMS (accelerator mass spectrometry) with the tandem accelerator at the Institute of Particle Physics at the Swiss Federal Institute of Technology Zurich (ETH).

⁽²⁾Calibration (2σ range) was carried out applying Intercal98-calibration curve (Stuiver and Reimer, 1993).

⁽³⁾Position of the dated sample relative to the event horizon.

⁽⁴⁾Derived from C¹⁴ data.

⁽⁵⁾Ages are rounded to the decade.

⁽⁶⁾Laacher See Tephra (LST), radiocarbon dated by Hajdas et al. (1995).

⁽⁷⁾Dates by Lister (1988).

References

- Bakun, W.H., and Wentworth, C.M., 1997, Estimating earthquake location and magnitude from seismic intensity data: *Bulletin of the Seismological Society of America*, v. 87, p. 1502-1521.
- Fäh, D., Giardini, D., Bay, F., Bernardi, F., Braunmiller, J., Deichmann, N., Furrer, M., Gantner, L., Gisler, M., Isenegger, D., Jimenez, M.J., Kastli, P., Koglin, R., Masciadri, V., Rutz, M., Scheidegger, C., Schibler, R., Schorlemmer, D., Schwarz-Zanetti, G., Steimen, S., Sellami, S., Wiemer, S., and Wossner, J., 2003, Earthquake Catalogue Of Switzerland (ECOS) and the related macroseismic database: *Eclogae Geologicae Helvetiae*, v. 96, p. 219-236.
- Hajdas, I., IvyOchs, S.D., Bonani, G., Lotter, A.F., Zolitschka, B., and Schluchter, C., 1995, Radiocarbon age of the Laacher See Tephra: 11,230+/-40 BP: *Radiocarbon*, v. 37, p. 149-154.
- Kelts, K., and Hsu, K.J., 1980, Resedimented facies of 1875 Horgen slumps in Lake Zurich and a process model of longitudinal transport of turbidity currents: *Eclogae Geologicae Helvetiae*, p. 73; 1, Pages 271-281.
- Lister, G.S., 1988, A 15,000-year isotopic record from Lake Zuerich of deglaciation and climatic change in Switzerland: *Quaternary Research*, v. 29, p. 129-141.
- Monecke, K., Anselmetti, F.S., Becker, A., Sturm, M., and Giardini, D., 2004, The record of historic earthquakes in lake sediments of Central Switzerland: *Tectonophysics*, v. 394, p. 21-40.
- Stuiver, M., and Reimer, P.J., 1993, Extended C-14 Data-Base and Revised Calib 3.0 C-14 Age Calibration Program: *Radiocarbon*, v. 35, p. 215-230.